EPD Congress 2016
Edited by: Antoine Allanore, Laura Bartlett, Cong Wang, Lifeng Zhang, and Jonghyun Lee
TMS (The Minerals, Metals & Materials Society), 2016

HYDROGEN REDUCTION KINETICS OF MECHANICALLY ACTIVATED MAGNETITE CONCENTRATE

Ricardo Morales-Estrella[1], Juan Ruiz-Ornelas[1], Yousef Mohassab[2], Noemi Ortiz-Lara[1], and Hong Yong Sohn[2]

[1] Instituto de Investigación en Metalurgia y Materiales, Universidad Michoacana de San Nicolás de Hidalgo, Morelia, Michoacán, C.P. 58030, México.
[2] Department of Metallurgical Engineering, University of Utah, Salt Lake City, UT 84112, USA.

Keywords: Hydrogen reduction, magnetite, mechanical activation, reduction kinetics.

Abstract

The effect of mechanical activation on the reduction kinetics of magnetite concentrate by hydrogen was studied. The magnetite concentrate was milled for 8 h using a planetary mill. After the milling process, the average particle size was reduced from 14 to 4.4 μm resulting in a lattice microstrain of 0.30. Thermogravimetric experiments were conducted to focus on the chemical reaction as the rate controlling factor by eliminating external mass transfer effects and using a thin layer of particles to remove interstitial diffusion resistance. The onset temperature of reduction was decreased due to the mechanical activation, and the degree of conversion was decreased by sintering of particles which was confirmed by SEM analyses. In view of the results, a reaction rate expression is discussed from which the activation energy is calculated.

Introduction

The gaseous reduction of iron oxides is a complex heterogeneous reaction in which the intrinsic rate mechanisms depend upon many parameters such as temperature, type of gaseous reactant, and particle size. There is, therefore, extensive research focused on different oxides reduced under different conditions which often lead to discrepancies among published work. Pineau *et al*.[1] studied the reduction of synthetic magnetite by hydrogen in the temperature range of 483 - 1223 K. They used about 100 mg of particles with 10 - 20 μm in diameter. The Arrhenius plot revealed three distinct slopes from which they obtained different apparent activation energies. That is, 200 kJ/mol, 71 kJ/mol and 44 kJ/mol at $T < 523$ K, $523 K < T < 663$ K and $T > 663$ K, respectively. Pourghahramani and Forssberg [2] investigated the effect of mechanical activation on the hydrogen reduction of high purity hematite using 95 mg of sample and a hydrogen flow rate of 100 mL/min. They reported a decrease of 90 K in the onset of the reducing temperature with respect to the non-activated sample. In addition, wüstite phase was not detected as an intermediate phase during nonisothermal experiments with heating rates of 10 to 15 K/min. Under thermodynamic equilibrium, wüstite is an unstable phase below 843 K; however, as shown in Ref. [3], wüstite could be an intermediate phase during the reduction of hematite by hydrogen below 843 K under irreversible thermodynamic conditions. Research of industrial interest on iron oxides is mostly carried out in the form of pellets or sinter. Recently, Wang and Sohn [4] investigated the reduction kinetics of fine magnetite concentrates using a novel process for rapid reduction; they developed a rate expression for the reduction process and obtained an activation energy value of 463 kJ/mol in the temperature range of 1243 - 1673 K. The objective

of this work was to study the reduction kinetics of mechanically activated magnetite concentrates by hydrogen. The experimental conditions were set up to obtain the rate of the chemical reaction as the rate controlling factor. The results were compared to non-activated samples and a rate expression was established for the reduction of both activated and non-activated samples.

Experimental

Materials

Magnetite concentrate from the Mesabi Range of the U.S. was used as the solid reactant in this study and it is composed of 0.688, 0.041, and 0.271 of mass fractions of total iron, gangue, and oxygen, respectively. Argon and hydrogen gases, with 99.999% purity, were used in the thermogravimetric experiments.

Mechanical Activation

Mechanical activation of magnetite concentrate was induced by milling in a planetary ball mill (Restch, PM400) at 300 rpm. Stainless steel balls of 10 mm in diameter were used as the grinding media; the ball-to-powder weight ratio was kept at 10:1.

Characterization

The particle size distribution of as-received and milled particles was obtained by Dynamic Light Scattering (DLS) using a Coulter LS 100Q apparatus. The morphology of the samples was characterized using a JEOL 6400 scanning electron microscope (SEM) with a NORAN-EDS attachment. X-ray analyses were performed using a Bruker D8 Advance powder diffractometer with Bragg-Brentano geometry. The Bragg peaks of samples were recorded at 40 mA, 40 kV with a step size of 0.02 degree and 5 s per step using Cu-Kα radiation and a nickel filter to suppress fluorescence. The lattice strain of milled samples was calculated using TOPAS software provided by Bruker Corporation.

Isothermal reduction was carried out using a vertical thermogravimetric unit (Setaram, Setsys Evolution 16/18, France) having a detection limit of 0.03 μg. The balance is controlled by a PC through an interface. An Al_2O_3 crucible, with 8 mm inner diameter and 1 mm inner height, was used to hold the magnetite concentrate. To avoid particle agglomeration, a drop of alcohol was used to evenly disperse the sample on the bottom surface of the crucible. The temperature of the furnace was controlled by a Pt-Pt/13% Rh (S-type) thermocouple placed just below the crucible. The themogravimetric cycle began by heating the sample up to the reducing temperature at a heating rate of 20 K/min under helium gas with a constant flow of 15 mL/min. When the sample temperature was stabilized, the helium gas flow was stopped and hydrogen gas was introduced and kept at a constant flow until the sample weight loss remained unchanged. The mass change during TGA experiments was recorded at 1 s intervals. All experiments were corrected against the noise of the hydrogen gas velocity on the sample by running blank experiments under identical conditions. Preliminary reduction experiments were performed to establish the optimal parameters to obtain the rate of the chemical reaction as the rate controlling factor.

Results and Discussion

Magnetite concentrates were subjected to different milling times to both decrease particle size and introduce micro strain. Thus, Figure 1 shows that after two hours of milling time, the mean particle size seems to remain unchanged. It can be expected that after the initial particles fracture into smallest particles, the repeated mechanical deformations caused by high energetic ball–powder–ball and ball–powder–chamber collisions would introduce micro strain into the lattice. The micro strain for samples milled at different times was calculated using TOPAS software and is shown in Figure 2. From the above results, the sample milled for 8 hours was used to study the effect of mechanical activation on the reduction kinetics. For direct comparison, the as-received concentrate was also studied under similar reducing conditions.

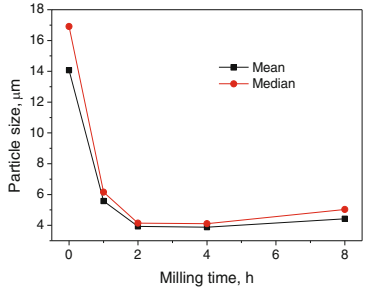

Figure 1. Particle size of magnetite concentrates as function of milling time.

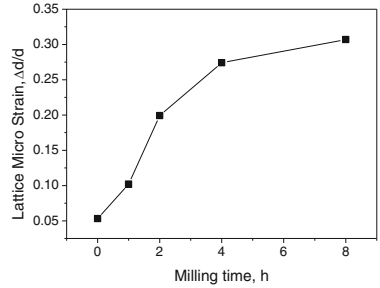

Figure 2. Lattice micro strain as function of milling time for the magnetite concentrate used in this work.

The particle size distribution of the two concentrate powders used in this work was measured and the results are shown in Figure 3. It can be seen that the milling process not only decreases the particle size but also narrows its distribution to a significant extent. The mathematical models for heterogeneous gas-solid reactions describe that the reaction rate depends on the radius of the spherical particle and therefore a constant particle size in the system is usually assumed. R. Morales *et al*. [5] took into account the range of particle size distribution in a rate expression for the chemical reaction showing negligible impact on the calculation of the activation energy.

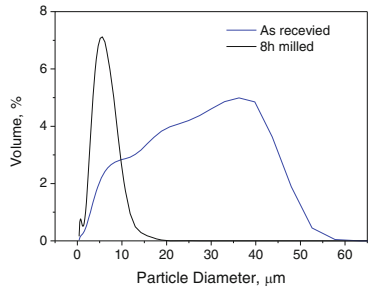

Figure 3. Particle volume distribution for magnetite concentrates.

It has been reported that the mechanical activation of hematite intensifies its thermal reactivity with hydrogen gas [2]. To verify whether the milled magnetite concentrate is able to decrease its onset temperature of reduction, nonisothermal experiments were performed for milled and as-received samples under predetermined conditions. The first derivative of each nonisothermal reduction curve was plotted against temperature in Figure 4 to show the onset temperature of reduction.

Figure 4 a) depicts earlier stages of reduction where the reactivity of the concentrate increases as the milling time is increased. It is to be noted that all curves show a discontinuity between 650 K and 665 K which correspond to $X < 0.1$. This behavior indicates that an intermediate phase is likely to be occurring. Although the Fe-O equilibrium diagram shows that wüstite is stable at temperatures above 843 K, the current experimental set up allows a constant removal of oxygen from the system leading to a nonequilibrium process in which case the wüstite phase could be present as a transitory phase. Note that the fraction of reduction at which the discontinuity occurs is lower than the theoretical value of X for the reduction of magnetite to wüstite, namely, 0.25. However, during the nonisothermal process, as temperature increases, the unstable wüstite phase is likely to get reduced to metallic iron before the reduction of magnetite to wüstite is completed. Figure 4 b) shows the whole range of the reduction fraction; it is observed that at about 730 K (457 ^{o}C with $0.22 < X < 0.28$), the derivative tends to increase as the milling time is increased. Thereafter, at about 820 K (547 ^{o}C with $0.73 < X < 0.80$), the derivative value decreases sharply. This sudden decrease indicates a mass transfer aspect affecting the reaction rate which is likely to be triggered by the relatively large amount of sample used in addition with the late stage of reduction. It is more likely that the mechanical activation has a greater impact on the initial stage of reduction. It is thought that the energy supply by the milling would form a metastable magnetite phase with appreciable structural defects.

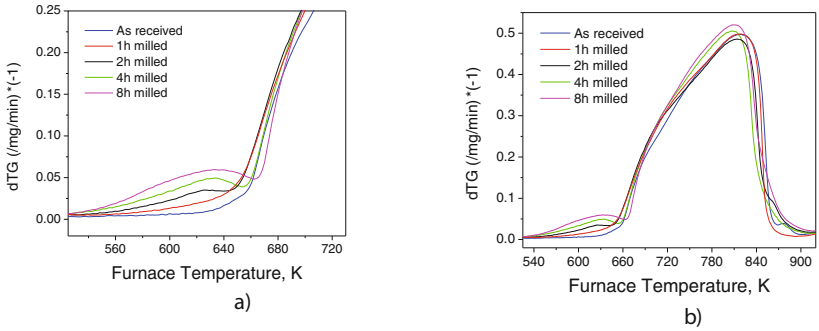

Figure 4. First derivative of the nonisothermal reduction experiments; a) derivative curves correspond to $0 < X < 0.25$, b) derivative curves correspond to $0 < X < 1$,

As mentioned earlier, the results shown in Figures 4 suggest a two-step reaction. This mechanism is currently being confirmed by the SEM and XRD analyses on quenched samples. Hence, the chemical reaction for the reduction of Fe_3O_4 by hydrogen gas can be represented as follow:

$$Fe_3O_4(s) + H_2(g) = 3FeO(s) + H_2O(g) \quad \Delta H = 63.7 \text{ kJ}; \; K_{eq} = 0.0117 \text{ at } 673 \text{ K} \qquad (1)$$

$$FeO(s) + H_2(g) = Fe(s) + H_2O(g)) \quad \Delta H = 16.6 \text{ kJ}; \; K_{eq} = 0.147 \text{ at } 673 \text{ K} \qquad (2)$$

For simplicity, FeO represents the nonstoichiometric nature of wüstite ($Fe_{1-x}O$). The milled concentrate was tested to find the optimal experimental parameters that lead to the chemical reaction as the slowest mechanism. Thus, to observe the effect of diffusion through the particles, the weight of the sample was varied as shown in Figure 5. The fractional reduction, X, was defined as the ratio of the instant weight loss, ΔWt, over the theoretical final weight loss, $\Delta W\infty$, corresponding to the loss of four oxygen atoms per Fe_3O_4 unit. It can be seen that from about 4 mg and below the reaction rate seems to remain constant. It should be remarked that 2 mg of powder did not cover the whole surface area of the crucible; therefore, 2 mg of powder was considered to study the reduction kinetics of magnetite concentrate by hydrogen.

Similarly, to examine the aspect of external mass transport in the gas phase, different flow rates of hydrogen were tested as shown in Figure 6. A hydrogen flow rate of 120 mL/min would avoid mass transfer issues on the reduction process.

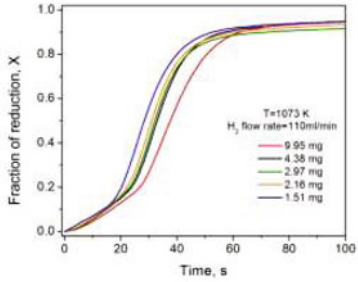

Figure 5. Effect of sample weight on the reduction reaction of 8-h milled magnetite concentrate.

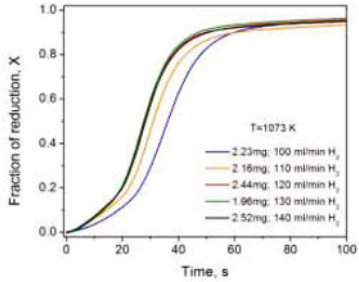

Figure 6. Effect of hydrogen flow rate on the reduction reaction of 8-h milled magnetite concentrate.

On the other hand, since the mean particle size for the 8-h-milled concentrate is about 4 μm and a very thin layer of loose particles was used, it is expected that the heat transfer would not be the controlling step even though the endothermic heats of Reactions (1) and (2) are appreciable.

From the above results, it is reasonable to assume that using about 2 mg of powder with a hydrogen flow rate of 120 mL/min, the rate-controlling step for Reactions (1) and (2) is most likely to be the chemical reaction at the reaction interface, except perhaps at the final stage of reduction.

Figure 7 shows the fractional reduction rate for the isothermal reduction of milled magnetite concentrate by hydrogen in the temperature range of 623 K to 1123 K. There is a detectable induction period at the beginning of the reaction which may indicate an intermediate reaction as aforementioned. As expected, the reduction rate increases with the increase in temperature being more evident in the temperature range of 673 K to 823 K. It is clearly seen that, at 623 K, the reduction rate is extremely slow. In fact, after 1800 s of processing the reduced fraction was estimated to be only 0.6. While at 1123 K, it only takes 45 s to reach a reduce fraction of 0.86. This low rate may indicate sintering of particles leading to a decrease in surface area.

It can also be noticed that at 973 K, the reduction rate is slightly slower than that at 873 K. This observation can be attributed to significant sintering of particles.

The isothermal reduction experiments of as-received concentrate are shown in Figure 8. It is observed that only the experiments conducted at 673 K, 723 K, and 773 K are more sensitive to temperature increase. This behavior is not uncommon distinct in chemical-reaction controlled processes. At higher temperatures, the increase in the reduction rate with temperature drops dramatically. Generally, all reduction curves in Figure 8 present a slower reduction kinetics compared with the milled concentrates, which is expected due to the larger particle size of the as-received ore.

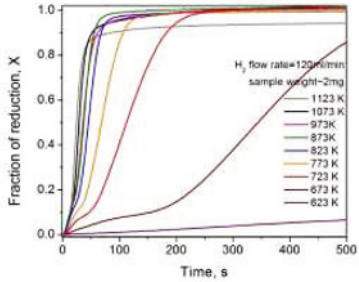

Figure 7. Effect of temperature on the reduction reaction of the 8-h milled magnetite concentrate.

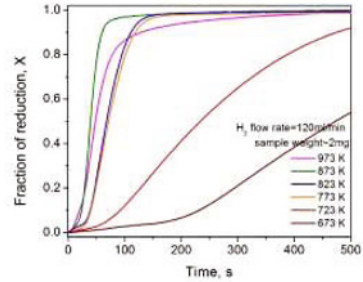

Figure 8. Effect of temperature on the reduction reaction of the as-received magnetite concentrate.

Figure 9 shows SEM images of milled particles and as-received particles before and after being reduced at 1123 K. Before the reduction process the as-received particles show an irregular and rectangular shape while the milled particles have a nearly spherical shape with tendency to form agglomerates. The difference in particle size between the two samples is very evident. The SEM images of both samples after being reduced at 1123 K reveal structures with less homogeneous porosity which can be attributed to sintering. The sintering effect was already elucidated in the reduction curves at higher temperatures as discussed earlier.

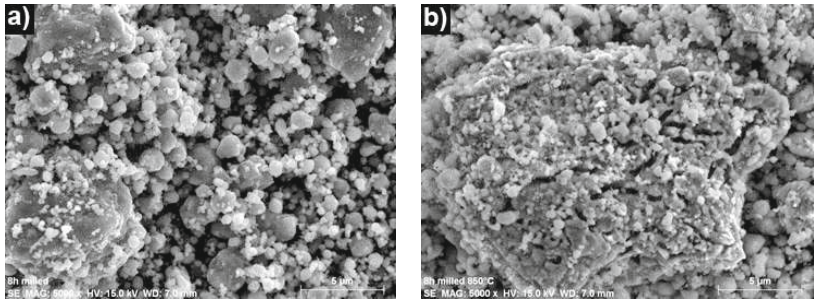

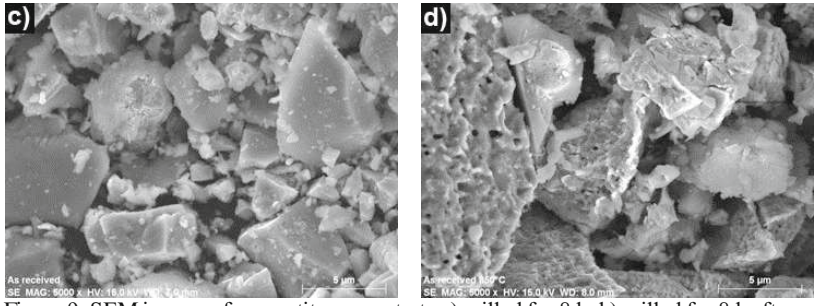

Figure 9. SEM images of magnetite concentrate a) milled for 8 h, b) milled for 8 h after being reduced at 1123 K, c) as-received, and d) as-received after being reduced at 1123 K.

The nucleation and grow kinetics has been found to describe the rates of reduction of iron oxide [6] and cuprous sulfide [7]. Recently, Wang and Sohn [4] used the nucleation and growth model to develop a rate expression for the hydrogen reduction of magnetite concentrates, in the temperature range of 1423 - 1673 K, by means of a novel gas-solid suspension set up. The nucleation and grow expression attributed to Avrami [8] is represented as:

$$[-\mathrm{Ln}(1-X)]^{1/m} = k_{app}\, t \tag{3}$$

where X is the fraction of reduction, t is the reaction time, m is a constant and k_{app} is the apparent rate constant which contains the dependence of the rate on gaseous reactant concentration and thus can be written as [9]:

$$k_{app} = b\, k\, f(\mathrm{C_{H2}}) \tag{4}$$

where b is the number of moles of solid reacted by one mole of gaseous reactant (b = 1 in this work), k is the intrinsic rate constant, C_{H2} is the hydrogen concentration in the bulk phase in mol/cm^3, and f designates the rate dependence on C_{H2}. All experiments were conducted at very excess driving force therefore the reverse reaction was not considered. Assuming a first-order reaction with respect to hydrogen concentration, namely $f(C_{H2}) = C_{H2}$, Equation (4) yields to $k = k_{app}/C_{H2}$. From Equation (3), It is seen that Ln[-Ln(1-X)] should be a linear function of Ln t with m as the slope and m Ln k_{app} as the intercept with the Ln t = 0 axis.

Figure 10 shows a plot of Ln[-Ln(1-X)] against Ln t for the results shown in Figure 8 with the isothermal data corresponding to $0.2 < X < 0.9$. The average value of the slopes obtained by regression analysis was 2.89 confirming that nucleation and grow products were three-dimensional. To obtain the intercept with the Ln t = 0 axis, and thus the value of k_{app}, a constant value of m = 3 was used throughout. Figure 11 a plot of Ln[-Ln(1-X)] against Ln t for the results shown in Figure 9. In this case, the average value of the slopes was 2.61 which is in accordance

with the less spherical particle shape observed in SEM images. For simplicity, a value of $m = 3$ was used to obtain the apparent rate constants.

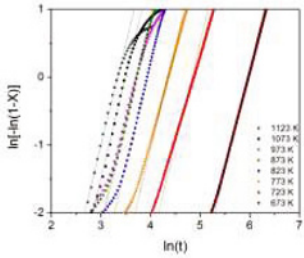

Figure 10. Plot of Ln[-ln(1-*X*)] *vs* Ln *t* from the results of Figure 8.

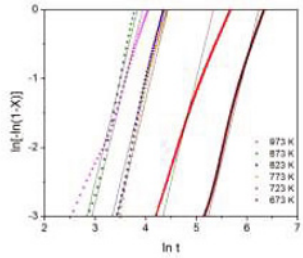

Figure 11. Plot of Ln[-Ln(1-*X*)] *vs* Ln *t* from the results of Figure 9.

Figure 12 shows the intrinsic rate constants as an Arrhenius plot. The experimental data seem to fit different consecutive slopes. Similar mode has been also reported in Ref. [1]. The rate constants, corresponding to higher temperatures, were left out from the calculation of the activation energy as it is likely to follow a different reduction mechanism. The computed values of the activation energy led to 67 kJ/mol and 80 kJ/mol for the mechanical activated concentrate and as-received concentrate, respectively. The activation energies thus obtained would correspond to the chemical reaction as the rate controlling as only those rate constants that were sensitive to temperature increase were considered. The difference in the activation energies should be attributed to the mechanical activation alone and not to the difference in particle size. A change in particle size can modify the rate constant at different temperatures but not the value of activation energy provided the system is controlled by the rate of the chemical reaction. Although the difference in activation energy does not appear to be significant, it should be born in mind that the equilibrium constant for Reaction (2) is less than one; therefore, the activation energy tends to be small and so is the difference in activation energies.

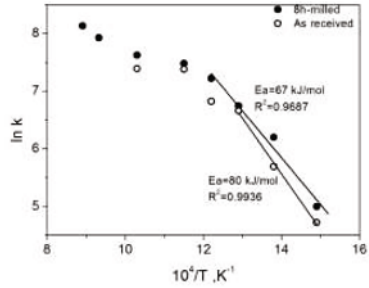

Figure 12. Arrhenius plots for the isothermal reduction of 8-h-milled and as-received magnetite concentrate.

Conclusions

In the present work, the mechanically activated concentrate with a lattice micro strain 0.30 showed an onset temperature of reduction 100 K lower than the as-received sample. Nonisothermal experiments suggest that the reduction of mechanically-activated magnetite concentrate may go through wüstite as transitory metastable phase for temperatures below 853 K. The activation energies were calculated based on the nucleation and grow model when the rate of chemical reaction is the controlling mechanism leading to 67 kJ/mol and 80 kJ/mol in the temperature range for the mechanically-activated concentrate and as–received concentrate, respectively. The rate of conversion for the hydrogen reduction of magnetite concentrate by hydrogen is given by:

$$dX/dt = 3 \cdot k \cdot [-\mathrm{Ln}(1-X)]^{2/3} \cdot (1-X) \cdot C_{H2} \quad (5)$$

with $k = 2.96\times10^{6}\cdot\exp(-8058/T)$ ($cm^3\cdot mol^{-1}\cdot s^{-1}$) for the 8-h-milled magnetite concentrate, and $k = 1.94\times10^{8}\cdot\exp(-9622/T)$ ($cm^3\cdot mol^{-1}\cdot s^{-1}$) for the as-received magnetite concentrate.

References

1. A. Pineau, N. Kanari and I. Gaballah, "Kinetics of reduction of iron oxides by H_2 Part II. Low temperature reduction of magnetite," Thermochimica Acta, 456 (2007), 75–88.
2. P. Pourghahramani and E. Forssberg, "Effects of mechanical activation on the reduction behavior of hematite concentrate," Int. J. Miner. Process, 82 (2007), 96–105.
3. A. Pineau, N. Kanari and I. Gaballah, "Kinetics of reduction of iron oxides by H_2 Part I. Low temperature reduction of hematite," Thermochimica Acta, 447 (2006), 89–100.
4. H. Wang and H.Y. Sohn, "Hydrogen Reduction Kinetics of Magnetite Concentrate Particles Relevant to a Novel Flash Ironmaking Process," Metall. Mater. Trans. B, 44.1 (2013), 133-145.
5. R. Morales, Du Sichen and S. Seetharaman, "Reduction Kinetics of Fe_2MoO_4 Fine Powder by Hydrogen in a Fluidized Bed," Metall. Mater. Trans. B, 34.10 (2003), 661-667.
6. Y. K. Rao, "Mechanism and the intrinsic rates of reduction of metallic oxides," Metall. Mater. Trans. B, 10 (1979), 243-255.
7. H. Y. Sohn and S. Won, "Intrinsic kinetics of the hydrogen reduction of Cu_2S," Metall. Mater. Trans. B, 16 (1985), 831-839.
8. M. Avrami, "Granulation, Phase Change, and Microstructure Kinetics of Phase Change. III," J. Chem. Phys., 9 (1941), 177-184.
9. H. Y. Sohn, "The law of additive reaction times in fluid-solid reactions," Metall. Mater. Trans. B, 9 (1978), 89-96.